

# SIMULTANEOUS BAND-WEIGHTING AND SPECTRAL UNMIXING FOR MULTIPLE ENDMEMBER SETS

Piyush Khopkar and Alina Zare

Department of Electrical and Computer Engineering  
University of Missouri  
Columbia, Missouri USA

## ABSTRACT

In this paper, the SimUltaneous Band-weighting and Spectral Unmixing for Multiple Endmember Sets (SUBSUME) which performs endmember extraction for multiple sets of endmembers, estimates proportion values, and assigns partition-specific band weights is presented. By incorporating simultaneous band weighting, input hyperspectral data is partitioned while focusing on spectral information from the wavelengths that provide the smallest error. Results are shown on two measured hyperspectral images.

**Index Terms**— Clustering, hyperspectral, piecewise convex, unmixing, band weighting, endmember.

## 1. INTRODUCTION

The goal of this paper is to perform simultaneous band weighting, endmembers estimation, and spectral unmixing for multiple endmember sets. In hyperspectral data, there is often highly correlated information in neighboring spectral bands. Also, irrelevant bands may degrade the performance of spectral unmixing methods. As a result, band weighting can aid hyperspectral unmixing and endmember estimation methods. Here, band weighting refers to a method for assigning weights to each band in hyperspectral data that indicate the relative degree of importance or contribution provided during unmixing.

Many endmember detection and spectral unmixing algorithms for hyperspectral data which rely on the *linear mixing model* (as shown in Equation 1) have been proposed in the literature [1, 2],

$$\mathbf{x}_i = \sum_{k=1}^M p_{ik} \mathbf{e}_k + \epsilon_i \quad i = 1, \dots, N \quad (1)$$

where  $N$  is the number of pixels in the image,  $M$  is the number of endmembers,  $\epsilon_i$  is an error term,  $p_{ik}$  is the proportion of endmember  $k$  in pixel  $i$ , and  $\mathbf{e}_k$  is the  $k^{th}$  endmember [1]. The proportions of this model satisfy the constraints in

$$p_{ik} \geq 0 \quad \forall k = 1, \dots, M$$

$$\sum_{k=1}^M p_{ik} = 1 \quad (2)$$

The vast majority of spectral unmixing methods search for a single set of endmembers to describe a hyperspectral scene and, as such, they assume the input hyperspectral data lie a single convex region. Therefore, these approaches cannot be appropriately applied to non-convex hyperspectral data. Many hyperspectral scenes are

non-convex. For example, consider a scene consisting of two distinct ground regions (e.g. urban and rural areas) composed of distinct materials or endmembers. The image spectra from each region will then only be mixtures of the endmembers associated with the corresponding region. Considering that each of these endmember sets define a convex region or simplex, then, the set of all image spectra will consist of a union of these convex regions. This union is may not be (and is unlikely to be) convex. To address this, several methods have been developed that represent hyperspectral imagery using a piece-wise convex representation [3, 4, 5, 6]. In these methods, hyperspectral data are represented using multiple sets of endmembers.

In this work, the piece-wise convex representation presented in [6] is extended to perform simultaneous band weighting using an approach motivated by the Simultaneous Clustering and Attribute Discrimination (SCAD) algorithm [7]. The SCAD algorithm performs simultaneous clustering and feature weighting. SCAD partitions input data into more meaningful clusters by focusing on the information provided by the most discriminating features. Similarly, this paper extends the Piece-wise Convex Multiple Model Endmember Detection (PCOMMEND) algorithm to incorporate simultaneous band weighting such that input hyperspectral data are partitioned by focusing on the bands providing the lowest reconstruction error. Thus, this method performs endmember extraction for multiple sets of endmembers, estimates proportion values for each input data point, and estimates partition-specific band weights.

A brief review of the PCOMMEND and SCAD algorithms are provided in Section 2. Section 3 describes the SUBSUME method. Section 4 presents results. Finally, Section 5 provides conclusion and discussion of future work.

## 2. REVIEW OF PCOMMEND AND SCAD ALGORITHMS

### 2.1. PCOMMEND

The PCOMMEND algorithm estimates endmember and proportion values by minimizing the objective shown in Equation 3.

$$J_p(\mathbf{E}, \mathbf{P}, \mathbf{U}) = \sum_{c=1}^C \left( \sum_{n=1}^N u_{cn}^q (\mathbf{x}_n - \mathbf{E}_c \mathbf{p}_{cn})^T (\mathbf{x}_n - \mathbf{E}_c \mathbf{p}_{cn}) \right. \\ \left. + \alpha \sum_{m=1}^{M-1} \sum_{k=m+1}^M (\mathbf{e}_{cm} - \mathbf{e}_{ck})^T (\mathbf{e}_{cm} - \mathbf{e}_{ck}) \right) \quad (3)$$

such that  $p_{cnm} \geq 0$ ,  $\sum_{m=1}^M p_{cnm} = 1$ ,  $u_{cn} \geq 0$  and  $\sum_{c=1}^C u_{cn} = 1 \quad \forall n$  where  $\mathbf{x}_n$  is a  $d \times 1$  column vector representing the  $n^{th}$  pixel,  $C$  is the number of endmember sets being estimated,  $\mathbf{p}_{cn}$  is the vector of proportion values associated with

pixel  $n$  for the  $c^{th}$  endmember set,  $\mathbf{E}_c$  is a  $d \times M$  matrix such that each column of  $\mathbf{E}_c$ ,  $\mathbf{e}_{cm}$ , is the  $d \times 1$  vector representing the  $m^{th}$  endmember in the  $c^{th}$  endmember set, weight  $u_{cn}$  is the membership value of the  $n^{th}$  data point in the  $c^{th}$  endmember set,  $\alpha$  is a fixed parameter used to balance the two terms of the objective, and  $q$  is a fixed parameter which controls the degree of sharing across endmember sets.

The first term of this objective is an error term computed using the squared Euclidean distance between each pixel and its estimate using the endmember and proportion values. The second term is used to constrain the size of each convex region by computing the squared Euclidean distance between each pair of endmembers in an endmember set. The membership values,  $u_{cn}$ , in the first term provide a fuzzy partitioning of the input scene by indicating the degree to which pixel  $n$  is in the  $c^{th}$  endmember set.

In PCOMMEND, endmembers, proportions and membership values are estimated using alternating optimization. All values are initialized and, then, the endmembers, proportions, and membership values are updated iteratively by minimizing the objective function above given the current estimates of all other parameters.

## 2.2. SCAD

The SCAD algorithm performs simultaneous clustering and feature weighting by minimizing the objective shown in Equation 4.

$$J_{scad}(\mathbf{C}, \mathbf{U}, \mathbf{V}) = \sum_{c=1}^C \sum_{n=1}^N u_{cn}^q \sum_{d=1}^D v_{cd} (x_{nd} - c_{cd})^2 + \sum_{c=1}^C \delta_c \sum_{d=1}^D v_{cd}^2 \quad (4)$$

where  $C$  is the number of clusters,  $N$  is the number of data points,  $u_{cn}$  is the membership values for the  $n^{th}$  data point in the  $c^{th}$  cluster,  $q$  is a fixed “fuzzifier” parameter controlling the degree of sharing across clusters,  $D$  is the number of dimensions/features of the input data,  $x_{nd}$  is the  $d^{th}$  feature of the  $n^{th}$  data point,  $c_{cd}$  is the  $d^{th}$  feature of the  $c^{th}$  cluster center,  $\delta_c$  is a parameter used to balance the terms of the objective, and  $v_{cd}$  is the feature weight for the  $d^{th}$  feature in cluster  $c$ . Furthermore, the membership values,  $u_{cn}$  and the feature weights,  $v_{cd}$  are constrained such that  $u_{cn} \in [0, 1]$ ,  $\sum_{c=1}^C u_{cn} = 1 \forall n = \{1, \dots, N\}$ ,  $v_{cd} \in [0, 1]$ , and  $\sum_{d=1}^D v_{cd} = 1 \forall c = \{1, \dots, C\}$ .

The SCAD objective consists of two terms. The first term follows the form of the fuzzy c-means clustering algorithm objective function [8] and is used to estimate cluster centers and a fuzzy partition of the input data with the addition of weighted feature values (through the inclusion of the  $v_{cd}$  weights for each dimension). The second term in the objective function is used to promote small feature weights (and, thus, is minimized when all feature weights are equal to  $\frac{1}{D}$ ). The SCAD parameters are estimated using alternating optimization.

## 3. SUBSUME

SUBSUME performs simultaneous endmember estimation, spectral unmixing and band weighting for multiple sets of endmembers by defining a objective function that combines the terms from the PCOMMEND and SCAD objectives. The objective function minimized

by the proposed approach is shown in Equation 5.

$$J(\mathbf{E}, \mathbf{P}, \mathbf{U}, \mathbf{V}) = \sum_{c=1}^C \left( \sum_{n=1}^N u_{cn}^q \sum_{d=1}^D v_{cd} (x_{nd} - \mathbf{E}_{cd} \mathbf{p}_{cn})^2 + \alpha \sum_{m=1}^{M-1} \sum_{k=m+1}^M (\mathbf{e}_{cm} - \mathbf{e}_{ck})^T (\mathbf{e}_{cm} - \mathbf{e}_{ck}) + \delta_c \sum_{d=1}^D v_{cd}^2 \right) \quad (5)$$

where  $u_{cn}$  is the membership value of the  $n^{th}$  data point in the  $c^{th}$  endmember set,  $q$  is a fixed parameter which controls the degree of sharing across endmember sets,  $v_{cd}$  is the band weight for the  $d^{th}$  band in end member set  $c$ ,  $x_{nd}$  is the  $d^{th}$  element of the  $n^{th}$  pixel,  $\mathbf{p}_{cn}$  is the vector of proportion values associated with pixel  $n$  for the  $c^{th}$  endmember set,  $\mathbf{E}_{cd}$  is a  $1 \times M$  vector containing the  $d^{th}$  band value for each of the  $M$  endmembers in set  $c$ ,  $\mathbf{e}_{cm}$  is the  $d \times 1$  vector representing the  $m^{th}$  endmember in the  $c^{th}$  endmember set,  $\delta_c$  and  $\alpha$  are fixed parameter values used to balance the terms of the objective function.

This objective function is minimized using alternating optimization. All values are initialized and, then, the endmembers, proportions, membership values, and band weights are updated iteratively. The update equation for the membership values is found by solving  $\frac{\partial J}{\partial u_{cn}} = 0$  after adding a Lagrange multiplier term to enforce the sum-to-one constraint,

$$u_{cn} = \frac{1}{\sum_{k=1}^C \left( \sum_{d=1}^D v_{kd} (x_{nd} - \mathbf{E}_{kd} \mathbf{p}_{kn})^2 \right)^{\frac{1}{q-1}}} \quad (6)$$

The update equation for the band weights is found to be,

$$v_{cd} = \frac{1}{D} + \frac{1}{2\delta_c} \sum_{n=1}^N u_{cn}^q \left[ \frac{\|\mathbf{x}_n - \mathbf{E}_c \mathbf{p}_{cn}\|_2^2}{D} - (x_{nd} - \mathbf{E}_{cd} \mathbf{p}_{cn})^2 \right] \quad (7)$$

The update equation for the endmembers is shown in Equation 8.

$$\mathbf{E}_{cd} = \left( \sum_{n=1}^N u_{cn}^q \mathbf{p}_{cn} \mathbf{p}_{cn}^T + \alpha (I_{M \times M} - \mathbf{1}_{M \times M}) \right)^{-1} \times \left( \sum_{n=1}^N u_{cn}^q \mathbf{p}_{cn} x_{nd}^T \right) \quad (8)$$

where  $I_{M \times M}$  is an  $M \times M$  identity matrix and  $\mathbf{1}_{M \times M}$  is an  $M \times M$  matrix of ones. Minimizing the objective function,  $J$ , with respect to  $\mathbf{p}_{ij}$  by adding a Lagrange multiplier term to enforce the sum-to-one constraint and applying the Karush-Kuhn-Tucker (KKT) conditions to enforce the non-negativity constraints on the proportion values, results in the following update for the proportion values,

$$\mathbf{p}_{cn}^T = \left( 2\mathbf{u}_{cn}^q \sum_{d=1}^D \mathbf{E}_{cd} \mathbf{E}_{cd}^T \right)^{-1} \left( D\lambda_c \mathbf{1}_{M \times 1} + 2\mathbf{u}_{cn}^q \sum_{d=1}^D \mathbf{E}_{cd}^T \mathbf{x}_{nd} \right) \quad (9)$$

$$\text{where } \lambda_c = \frac{1 - 1_{1 \times M} \left( \sum_{d=1}^D \mathbf{E}_{cd} \mathbf{E}_{cd}^T \right)^{-1} \sum_{d=1}^D \mathbf{E}_{cd}^T \mathbf{x}_{nd}}{1_{1 \times M} \left( D\mathbf{u}_{cn}^q \sum_{d=1}^D \mathbf{E}_{cd} \mathbf{E}_{cd}^T \right)^{-1} \mathbf{1}_{M \times 1}}$$

Proportion values are clipped at zero and then renormalized following this update (as dictated by KKT conditions) to ensure that they are greater than zero and sum to one.

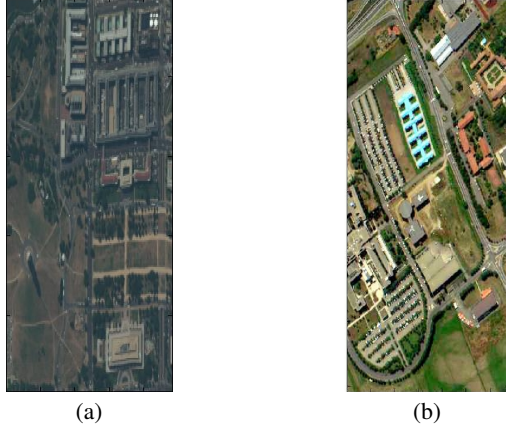


**Fig. 1.** RGB images of a subset of (a) HYDICE Washington DC Mall data and (b) ROSIS Pavia University data.

#### 4. EXPERIMENTAL RESULTS

In following, SUBSUME is applied to two measured hyperspectral image cubes. The first image is HYDICE Washington DC Mall data set. The second data set is the ROSIS Pavia University data. This data was acquired by ROSIS (Reflective Optics System Imaging Spectrometer) sensor during a flight campagin over city of Pavia, Italy. Figure 1 shows RGB images of a subset of Washington DC Mall data and ROSIS Pavia University data.

##### 4.1. HYDICE Washington DC Mall data set

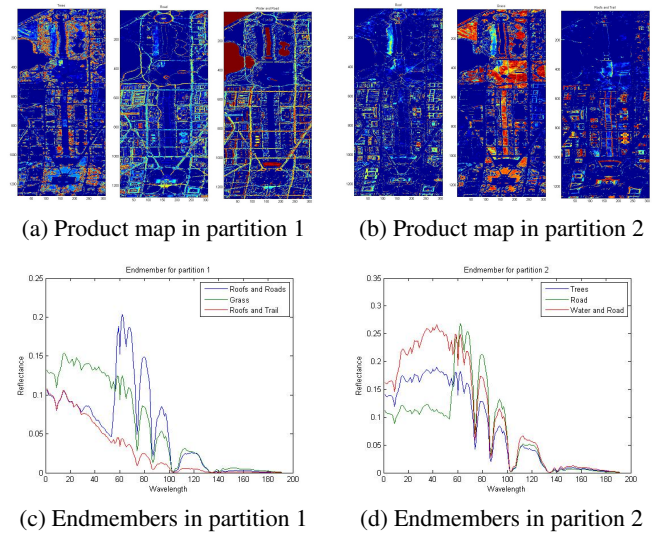
The HYDICE Washington DC Mall data set was collected over the Washington DC Mall area. The sensor system used for capturing the data measured pixel responses in 210 bands in the  $0.4$  to  $2.4\mu\text{m}$  region of the visible and infrared spectrum. Due to the opacity of the atmosphere in bands falling in  $0.9$  and  $1.4\mu\text{m}$  range, the data set has been reduced to 191 bands. The image has  $1208 \times 307$  pixels. The data includes the following ground cover types: roof, road, vegetation, sidewalk, water and shadow.

For comparison, SUBSUME and PCOMMEND were applied to the subset of the data with parameter settings of  $C = 2$ ,  $M = 3$ ,  $\alpha=0.005$ , and  $q=2$ . These values were determined manually after multiple runs of each algorithm across a range of parameter values. The best result (identified by having a qualitatively well separated class of endmembers) from each method are shown here.

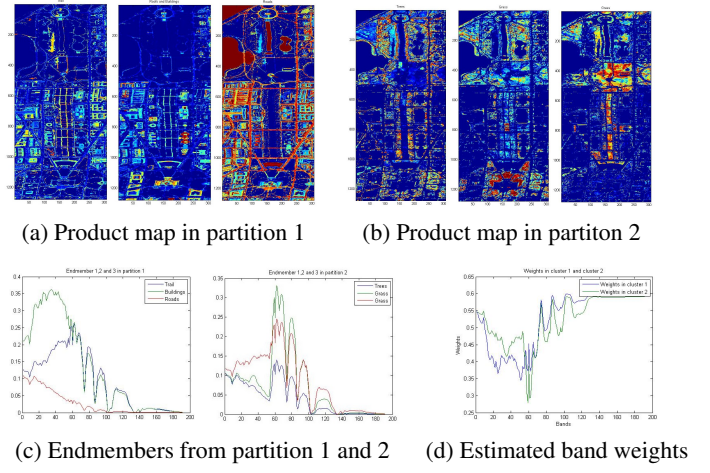
Figure 2 displays the estimated proportion maps scaled by the estimated membership values found using PCOMMEND. Figure 2 also shows the estimated endmembers for the two partitions.

Figure 3 shows the estimated proportion maps scaled by the estimated membership values, the estimated endmembers, and the estimated feature weights for both partitions found using the SUBSUME algorithm.

When comparing SUBSUME and PCOMMEND results, it can be seen that, with the inclusion of the band weights, SUBSUME is able to place all vegetation into a single convex region. In contrast, PCOMMEND splits vegetation across partitions. Note that in both results, water is combined with asphalt/road. This is due to the both materials having a flat spectral signature with small values.



**Fig. 2.** Weighted proportion maps estimated by PCOMMEND on Washington DC Mall data where (a) corresponds primarily to vegetation/trees, road and water, respectively, from partition 1 and (b) corresponds to roof, vegetation/grass and roof/sidewalk, respectively, from partition 2. Sub-figure (c) shows the estimated endmembers from partition 1 and (d) shows the estimated endmembers from partition 2.



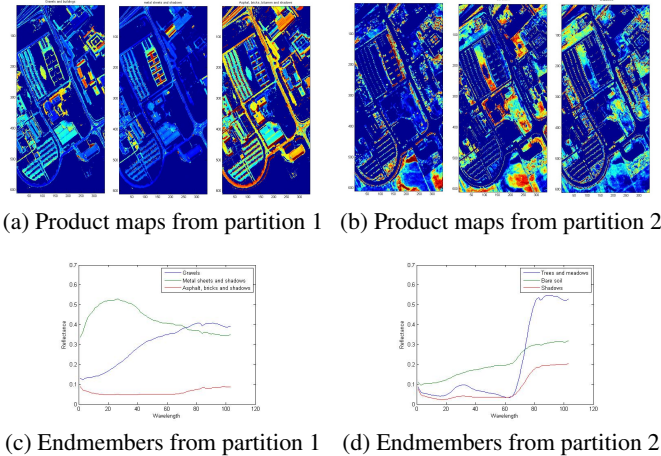
**Fig. 3.** Weighted proportion maps estimated by SUBSUME on Washington DC Mall data where (a) corresponds to roof, sidewalk, roads and water from partition 1 and (b) corresponds primarily to vegetation from partition 2. Sub-figure (c) shows the estimated endmembers from each partition, and (d) shows the estimated band weights for each partition.

##### 4.2. ROSIS Pavia University Data set

The Pavia university data was acquired by ROSIS sensor on July 08, 2002. The hyperspectral data cube used is  $610 \times 340$  pixels with 103 spectral bands. The data was collected over the wavelength range of  $0.43$  to  $0.85 \mu\text{m}$  and contains several materials including trees, asphalt, bricks, bitumen, tile, shadow, meadow, and soil [9].

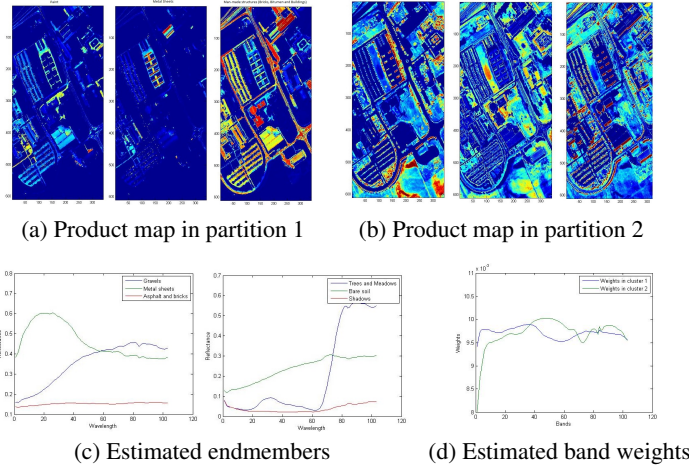
PCOMMEND and SUBSUME were run over a range of values for  $\alpha$ ,  $\delta$  (in case of SUBSUME) and  $q$ . The best results (manually identified by having qualitatively well separated class of endmembers) from each method are shown here.

Figure 4 displays the results using PCOMMEND on the Pavia data with parameter values of  $C = 2$ ,  $M = 3$ ,  $\alpha = 0.001$ , and  $q = 2$ .



**Fig. 4.** Weighted proportion maps estimated by PCOMMEND on Pavia data where (a) corresponds to bare soil/gravel, metal sheets, and man-made material, (b) corresponds to meadows, bare soil, and shadow, and (c) and (d) show estimated endmembers.

Figure 5 displays the SUBSUME results using parameters values of  $C = 2$ ,  $M = 3$ ,  $\alpha = 0.005$  and  $\delta = 1000$ .



**Fig. 5.** Weighted proportion maps estimated by SUBSUME algorithm on Pavia data where (a) corresponds to painted metal sheets and man-made material and (b) corresponds to trees-meadows, bare soil and shadows. Sub-figure (c) displays the estimated endmember spectra and (d) shows the partition-specific band weights.

When comparing these results, it can be observed that PCOMMEND combines some man-made and natural materials into a single

endmember. In particular, bare-soil and gravel/pavement are combined into a single endmember. In contrast, SUBSUME is able to distinguish between these materials.

## 5. CONCLUSION AND FUTURE WORK

The SUBSUME algorithm extends PCOMMEND and SCAD algorithm by estimating partition-specific band weights. The proposed approach performs band weighting, endmember estimation and spectral unmixing simultaneously such that endmembers and proportion values are estimated using the weighted band values. Results indicate that SUBSUME is effective at distinguishing between distinct materials and grouping similar materials across endmembers and partitions. Future work will include investigation into estimation of sparse band weights such that dimensionality reduction can be performed. Also, future work will include investigation into additional band-weight regularization terms such as partition-specific band weights that aid in distinguishing between endmember spectral signatures.

## 6. REFERENCES

- [1] N. Keshava and J. F. Mustard, "Spectral unmixing," *IEEE Signal Processing Magazine*, vol. 19, pp. 44–57, 2002.
- [2] J. M. Bioucas-Dias, A. Plaza, N. Dobigeon, M. Parente, Q. Du, and P. Gader, "Hyperspectral unmixing overview: Geometrical, statistical, and sparse regression-based approaches," *IEEE Journal of Selected Topics in Applied Earth Observations and Remote Sensing*, vol. 5, no. 2, pp. 354–379, April 2012.
- [3] A. Zare, *Hyperspectral Endmember Detection and Band Selection using Bayesian Methods*, Ph.D. thesis, University of Florida, 2009.
- [4] A. Zare and P. Gader, "PCE: Piece-wise convex endmember detection," *IEEE Transactions on Geoscience and Remote Sensing*, vol. 48, no. 6, pp. 2620–2632, Jun. 2010.
- [5] A. Zare, P. Gader, and G. Casella, "Sampling piecewise convex unmixing and endmember extraction," *IEEE Transactions on Geoscience and Remote Sensing*, 2012.
- [6] A. Zare, P. Gader, O. Bchir, and H. Frigui, "Piecewise convex multiple-model endmember detection and spectral unmixing," *IEEE Transactions on Geoscience and Remote Sensing*, 2012.
- [7] H. Frigui and O. Nasraoui, "Simultaneous clustering and attribute discrimination," in *Fuzzy Systems, 2000. FUZZ IEEE 2000. The Ninth IEEE International Conference on*, may 2000, vol. 1, pp. 158 –163 vol.1.
- [8] J. C. Bezdek, *Pattern Recognition with fuzzy objective function algorithm*, Plenum Press, 1981.
- [9] S. Holzwarth, A. Muller, M. Habermeyer, R. Richter, A. Haußold, S. Thiemann, and P. Strobl, "HySens - DAIS 7915/ ROSIS imaging spectrometers at DLR," in *3rd EARSeL Workshop on Imaging Spectroscopy*, May 2003.